

Chiral Sum Frequency Generation for *In Situ* Probing Proton Exchange in Antiparallel β -Sheets at Interfaces

Li Fu[†], Dequan Xiao[†], Zhuguang Wang, Victor S. Batista^{*}, and Elsa C. Y. Yan^{*}

Department of Chemistry, Yale University, 225 Prospect Street, New Haven, CT 06520

^{*}Corresponding authors [†]Equal Contribution

Emails: elsa.yan@yale.edu, victor.batista@yale.edu

I. SFG setup

The broad-bandwidth SFG spectrometer contains a 6-W regenerative amplifier seeded by a 120-fs 1.9-W Ti:sapphire oscillator (Mai Tai, Spectra-Physics) and pumped by two Nd:YLF pump lasers (16 W, Empower, Spectra-Physics). One half of the amplifier output (3 W) pumps an OPA (TOPAS, Spectra-Physics) to generate a 120-fs pulsed IR beam. The other half (3W) enters a pulse shaper to yield ~ 2 ps pulses to a narrow bandwidth of ~ 7 cm^{-1} . The pulse shaper consists of a grating, a planoconvex cylindrical lens, and a homemade slit. The 800 nm beam has an incident angle of 56° and the IR beam has an incident angle of 69° . The reflected SFG signal is filtered, focused onto the slit of the monochromator (SP-2558, Princeton Instruments), and detected by a CCD (Spec-10:400BR/LN, Princeton Instruments).

II. The amide II and amide II' bands of LK₇ β at the air/water interfaces.

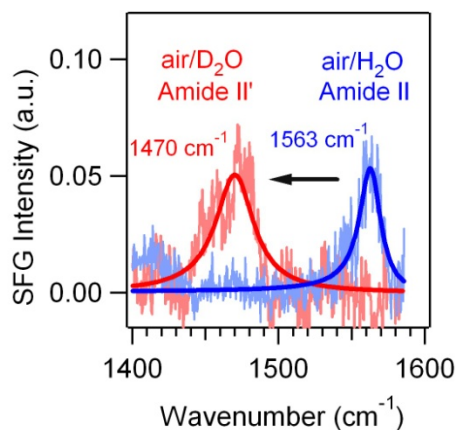


Figure S1. The cSFG spectrum of LK₇ β at the air/water interface in the region of 1300-1600 cm^{-1} .

Figure S1 shows the amide II/amide II' band of the LK₇ β at the air/H₂O and air/D₂O interfaces. The experimental conditions were the same as we obtained the N-H/N-D spectra. The amide II mode is a combination of the N-H in-plane bending and the C-N stretch. The H-to-D exchange converts the amide

II mode into a largely C-N stretch mode, shifting the frequency from 1563 cm^{-1} down to 1470 cm^{-1} , which is termed as the amide II' mode.

Table S1. The fitting parameter of Figure S1.

Spectrum Figure S1	Fitting parameters	Values
<i>Amide II</i>	χ_{NR1} (a.u.)	-0.014 ± 0.003
	ω_1 (cm^{-1})	1563 ± 0.3
	A_1 (a.u.)	2.03 ± 0.08
	Γ_1 (a.u.)	8.8 ± 0.4
<i>Amide II'</i>	χ_{NR2} (a.u.)	-0.044 ± 0.005
	ω_2 (cm^{-1})	1470 ± 0.5
	A_2 (a.u.)	2.76 ± 0.12
	Γ_2 (a.u.)	12.2 ± 0.6

III. Supplementary discussion: spectral analyses and *ab initio* calculations

The chiral N-H spectrum (Figure 2A) shows a shoulder peak at 3178 cm^{-1} , while the chiral N-D spectrum (Figure 2A) shows a shoulder peak at 2470 cm^{-1} . In the main text, we have discussed the assignment of the 3178- cm^{-1} peak to the Fermi resonance of combination band of amide I and amide II with N-H stretch and the 2470- cm^{-1} peak to the Fermi resonance of a combinational band of C-N stretch and N-D in-plane bending with N-D stretch. In the discussion, we have eliminated the possibilities of assigning the peaks to the amide I/amide II overtones, and the free N-H groups exposed to the solvent environment. Here, we provide the rationale of eliminating these possibilities.

We started by exploring the assignments of the shoulder peaks to Fermi resonance of the amide II overtone with the N-H/N-D stretch. First, we focus on the shoulder peak (3178 cm^{-1}) in the N-H spectrum. Traditionally, the N-H stretch vibrations in proteins are often assigned to the amide A (3300 cm^{-1}) and amide B modes (3070 cm^{-1}). The amide B mode is due to the Fermi resonance of the amide II overtone with the N-H stretch, where the amide II band (~ 1560 cm^{-1}) is mainly a combination of the N-H in-plane bending and the C-N stretch. However, the B mode frequency (~ 3070 cm^{-1}) does not match with the experimentally observed peak at 3178 cm^{-1} . Thus, the 3178- cm^{-1} peak cannot be assigned to the amide B. Second, we focus on the shoulder peak (2470 cm^{-1}) in the N-D spectrum. The isotopic substitution of N-H to N-D lowers the frequency of N-D in-plane bending so that it no longer couples with the C-N stretch. Thus, deuteration of the peptide N-H converts the amide II mode into a largely C-N stretch mode (also named as amide II' mode) at ~ 1460 -1490 cm^{-1} , whose overtone is no longer in Fermi resonance with the N-D stretch.⁴³ The frequency of the amide II' is indeed confirmed by our cSFG spectrum showing the peptide C-N stretch of LK₇ β at the air/D₂O interface at 1470 cm^{-1} (Figure S1).

After eliminating the possible assignment to Fermi resonance of the amide II overtone with the N-H/N-D stretch, we examined the possibility of assigning the 3178- cm^{-1} shoulder peak (Figure 2A) to the amide I overtone. According to our *ab initio* (B3LYP/6-31g*) anharmonic vibrational analysis for a model system of amide bond, N-methylacetamide (NMA), using the Gaussian 09 program (see Section V), the anharmonic constant of amide I band is -8.9 cm^{-1} . Based on this value, the overtone band of amide I (1620 cm^{-1} observed experimentally, Figure 1) should be 3222 cm^{-1} (i.e. $2 \times 1620 - 2 \times 8.9 = 3222$), which is higher than the observed shoulder peak at 3178 cm^{-1} . Hence, we eliminated the possibility of assigning the shoulder peaks to the amide I overtone.

Finally, we looked into the contribution of the free N-H groups that are exposed to the solvent environment. If the shoulder at $\sim 3178 \text{ cm}^{-1}$ is due to the free N-H groups pointing away from the antiparallel β -sheet strand and toward the solvent, its frequency would be sensitive to the changes in solvent environment. To test this, we obtained the N-H spectra of LK $_7\beta$ deposited on glass slides. The sample was prepared by adding one or two drops of LK $_7\beta$ solution on a glass slide, which was dried at room temperature for 24 hours. The 3178- cm^{-1} peak is found to remain at the same position (Figure. S2), suggesting that it is not likely due to the free N-H groups.

By eliminating the above possibilities, we concluded on the basis of the rationale presented in the main text that the shoulder peaks at 3178 cm^{-1} (Figure 2A) can be tentatively assigned to the Fermi resonance of the combination band of the amide I and amide II with the N-H stretch, and the shoulder peak at 2473 cm^{-1} (Figure 2B) can be tentatively assigned to the Fermi resonance of the combination band of the C-N stretch and N-D in-plane bending with the N-D stretch.

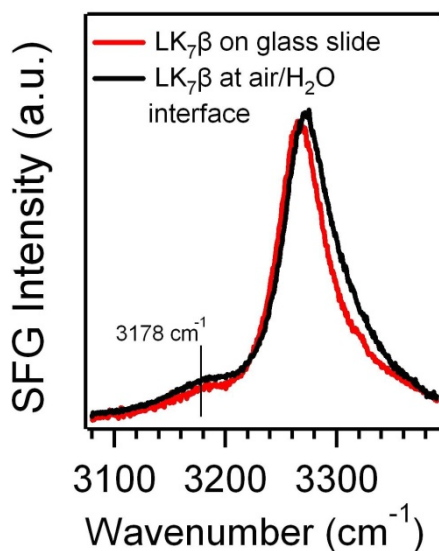


Figure S2. The cSFG spectrum of LK $_7\beta$ deposited on glass slide. A few drops of LK $_7\beta$ solution was deposited on the glass slide and dried for ~ 24 hours.

IV. Decreases in the N-H (N-D) signals upon the H-to-D (D-to-H) exchange.

In our experiments, we chose to monitor the kinetics of H/D exchange using increase of the N-D/N-H stretch signals rather than the decrease of the signals. When we examined the N-H (N-D) signals in the H-to-D (D-to-H) exchange process, and we indeed observed a substantial decrease of the N-H (N-D) signal towards the end of the exchange process (Figure S3). However, at the beginning of the exchange process, the N-H/N-D stretch signals fluctuate. Figure S4 shows the N-H signal during the H-to-D exchange. The N-H signal drops abruptly upon the addition of D₂O into H₂O and then recovers in the first 2-7 min. Then, the N-H signal gradually decreases. The initial fluctuation of signals makes it difficult to extract kinetic information.

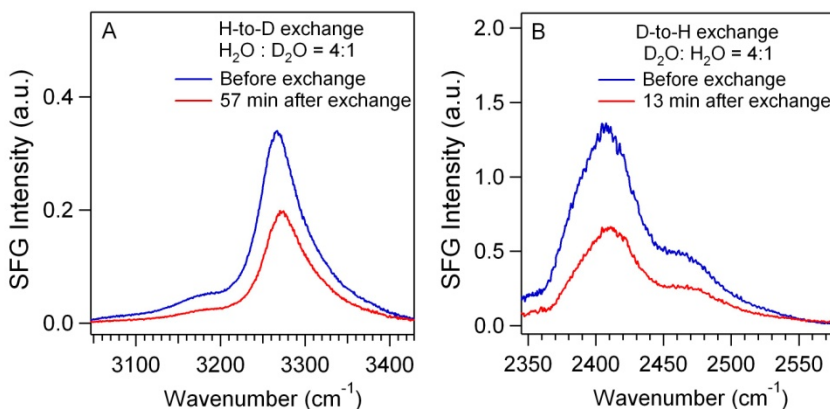


Figure S3. The decreased cSFG signals of the peptide N-H and N-D stretch of LK₇ β at the air/water interface upon H-to-D exchange and D-to-H exchange, respectively.

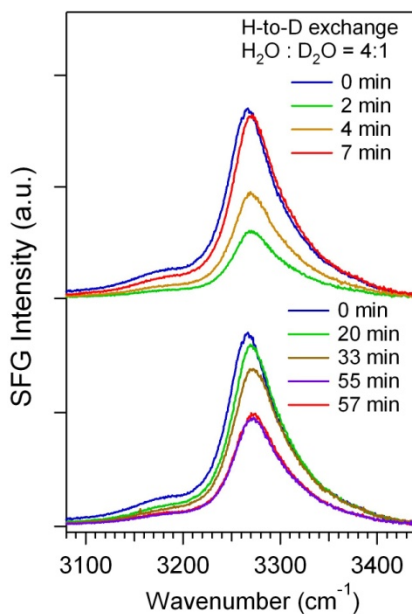


Figure S4. The time-dependent cSFG signals of the peptide N-H stretch of LK₇ β at the air/water interface upon the H-to-D exchange.

V. Computational details

(i) Simulation of SFG spectrum based on *ab initio* calculations.

The *psp* cSFG spectra were simulated based on the calculated β_{lmn} , using the following steps, which is similar to the simulation procedure used in our previous work.¹ First, the $\beta_{lmn,q}$ elements are computed by

$$\beta_{lmn,q} \propto \frac{\partial \alpha_{lm}}{\partial Q_q} \frac{\partial \mu_n}{\partial Q_q} \quad (\text{S1})$$

where α_{lm} and μ_n are the polarizability and dipole moment, respectively, and Q_q is the normal mode coordinate. Dipole derivatives of each vibrational mode were obtained using the keyword ‘iop(7/33=1)’ during a frequency calculation, and polarizability derivatives were obtained by performing the Raman vibrational analysis with the ‘polar’ keyword. The above calculations were performed using the Gaussian 09 program, as described previously.¹

For a particular set of orientation angles (ϕ, ψ, θ) , the 2nd-order susceptibilities of each normal mode ($\chi_{ijk,q}^{(2)}(\phi, \psi, \theta)$) were computed from $\beta_{lmn,q}$ via the Euler transformation using

$$\chi_{ijk,q}^{(2)} = N_s \sum_{l,m,n} R_{il} R_{jm} R_{kn} \beta_{lmn,q} \quad (\text{S2}),$$

where N_s is the number density of the chromophores, $R_{il} R_{jm} R_{kn}$ is the product of the Euler transformation matrix for the projection from the molecular coordinate (a, b, c) onto the lab coordinate (x, y, z) , and ϕ , θ , and ψ are Euler angles.¹ Second, we set $\theta = 0^\circ$ and $\psi = 0^\circ$ (i.e. assuming the β -sheets are aligned horizontally at the interface) and assume an isotropic distribution of β -sheets at the interface (i.e. $\phi = 0-2\pi$) and, the $\chi_{ijk,q}^{(2)}$ elements were obtained by averaging over $\chi_{ijk,q}^{(2)}(\phi, \psi, \theta)$ with a complete set of ϕ -angles (here, ϕ is sampled numerically every 5° from 0 to 360°) using

$$\chi_{ijk,q}^{(2)}(\psi) = \int_0^{2\pi} \chi_{ijk,q}^{(2)}(\phi, \psi, \theta = \pi/2) d\phi \quad (\text{S3})$$

Then, from $\chi_{ijk,q}^{(2)}(\psi)$, the effective susceptibilities $\chi_{psp,q}^{(2)}$ were calculated using

$$\chi_{psp,q}^{(2)} = L_{zyx}\chi_{zyx,q}^{(2)} - L_{xyz}\chi_{xyz,q}^{(2)} \quad (\text{S4})$$

where the Fresnel factors L_{zyx} and L_{xyz} , are $0.1927+i1.4739 \times 10^{-5}$ and $0.2157-i1.9184 \times 10^{-3}$, respectively, as determined by the geometry of the SFG setup. Subsequently, we introduced a Gaussian function to account for the inhomogeneous broadening effect on $\chi_{psp,q}^{(2)}$ for each normal mode. Thus, the overall effective susceptibility was calculated by

$$\chi_{psp}^{(2)}(\omega) = \sum_{q=1}^{N_s} g(\omega, \omega_q) \chi_{psp,q}^{(2)} \quad (\text{S5})$$

which is frequency-dependent. Finally, the SFG chiral spectrum was computed by

$$I_{psp}(\omega) = \left| \chi_{psp}^{(2)}(\omega) \right|^2 \quad (\text{S6})$$

(ii) Calculations anharmonic constant of the amide I bands.

We computed the anharmonic constant from N-methyl-amino acid (NMA) in gas phase to estimate the anharmonic constant of peptide unit in β -sheets. The anharmonic constant calculation for NMA was performed at the DFT (B3LYP/6-31g*) level using the Gaussian 09 program, with the keyword “frequency=anharmonic”.

(iii) Simulated SFG spectrum for N-deuterated peptides.

Following the procedure in (i), the *psp* cSFG spectrum for N-deuterated peptides (Scheme 1) was simulated in the range of 500-2800 cm^{-1} (Figure S5). The cSFG signals around 1000 cm^{-1} for the N-D bending mode is at least 18 times weaker than the cSFG peak of N-D vibration at 2420 cm^{-1} .

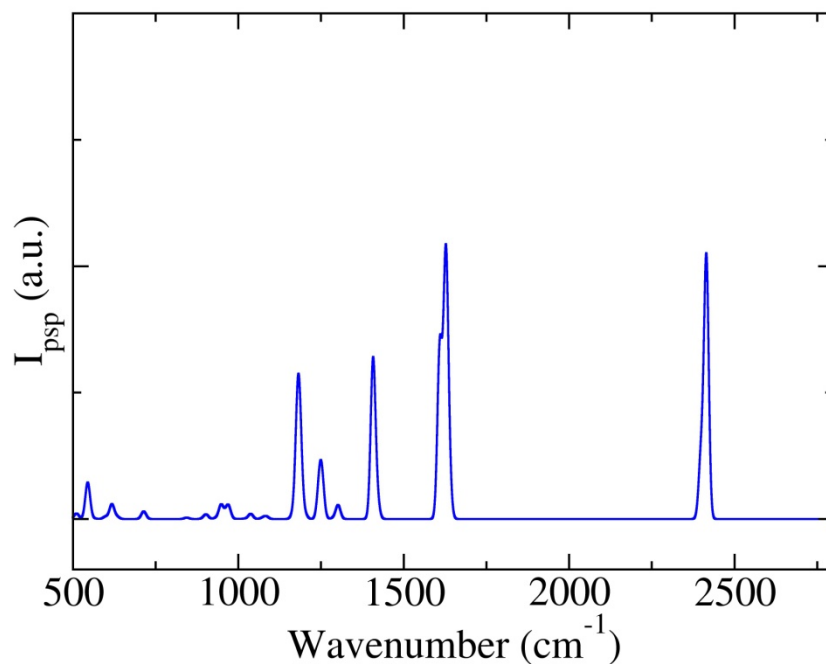


Figure S5. Simulated *psp* cSFG spectrum of the N-deuterated anti-parallel model peptide (Scheme 1 in the main text). The SFG signals are contributed mainly from the vibration normal modes of the amino acid units of N-H(D) groups 1-4 (Scheme 1 in the main text).

VI. Empirical analysis of kinetic data.

Since the time-dependent plots could be useful for comparing the differences in rates of H-to-D and D-to-H exchange, each spectrum presented in Figure 3 was fitted into Equation (1) to obtain the SFG field, which was then plotted it as a function of time and fitted into a stretched exponential function:

$$y = a\{1 - \exp[-(t/\tau)^\beta]\},$$

where τ reflect the empirical relaxation time. Figure S6 show the fitting results. The fitting for D-to-H with a ratio of D₂O:H₂O in 2:1 appears to be different from the rest of the data. This could be due to a fast relaxation ($\tau \sim 1.7$ min) in comparison with the time resolution of our experiment (1-min acquisition per spectrum). The overall analyses suggest that the relaxation time of the D-to-H exchange is about one order of magnitude faster than that of the H-to-D exchange.

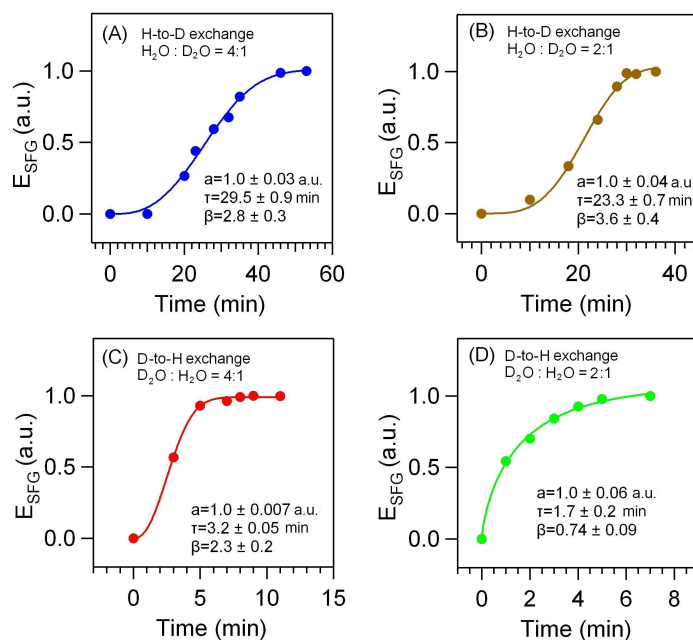


Figure S6. Stretched exponential fitting. (A) H-to-D exchange with $\text{H}_2\text{O}:\text{D}_2\text{O}$ 4:1, (B) H-to-D exchange with $\text{H}_2\text{O}:\text{D}_2\text{O}$ 2:1, (C) D-to-H exchange with $\text{D}_2\text{O}:\text{H}_2\text{O}$ 4:1, and (D) D-to-H exchange with $\text{D}_2\text{O}:\text{H}_2\text{O}$ 2:1.

Reference:

- (1) Xiao, D.; Fu, L.; Liu, J.; Batista, V. S.; Yan, E. C. Y. *J. Mol. Biol.* **2012**, 421, 537-547.